

MedSAGa: Few-shot Memory Efficient Medical Image Segmentation using Gradient Low-Rank Projection in SAM

Navyansh Mahla *

Indian Institute of Technology, Bombay
Mumbai, Maharashtra, India

210040106@iitb.ac.in

Shubh Gupta

Sardar Patel Institute of Technology, Mumbai
Mumbai, Maharashtra, India

shubh.gupta@spit.ac.in

Annie D'souza *

Indian Institute of Technology, Bombay
Mumbai, Maharashtra, India

20d070028@iitb.ac.in

Bhavik Kanekar

Indian Institute of Technology, Bombay
Mumbai, Maharashtra, India

bhavikkanekar@iitb.ac.in

Kshitij Sharad Jadhav

Indian Institute of Technology, Bombay
Mumbai, Maharashtra, India

kshitij.jadhav@iitb.ac.in

Abstract

The application of large-scale models in medical image segmentation demands substantial quantities of meticulously annotated data curated by experts along with high computational resources, both of which are challenges in resource-poor settings. In this study, we present the Medical Segment Anything Model with Galore (**MedSAGa**) where we adopt the Segment Anything Model (SAM) to achieve memory-efficient, few-shot medical image segmentation by applying Gradient Low-Rank Projection (**GaLore**) to the parameters of the image encoder of SAM. Meanwhile, the weights of the prompt encoder and mask decoder undergo full parameter fine-tuning using standard optimizers. We further assess MedSAGa's few-shot learning capabilities, reporting on its memory efficiency and segmentation performance across multiple standard medical image segmentation datasets. We compare it with several baseline models, including LoRA fine-tuned SAM (SAMed) and DAE-Former. Experiments across multiple datasets and these baseline models with different number of images for fine tuning demonstrated that the GPU memory consumption of MedSAGa is significantly less than that of the baseline models, **achieving an average memory efficiency of 66% more than current state-of-the-art (SOTA) models for medical image segmentation.** The combination of substantially lower memory requirements and comparable to SOTA re-

sults in few-shot learning for medical image segmentation positions MedSAGa as an optimal solution for deployment in resource-constrained settings.

1. Introduction

Image segmentation plays an important role in various aspects of healthcare, enabling precise analysis and diagnosis from medical imaging data such as MRI, CT scans, and ultrasound [21]. By accurately delineating anatomical structures or pathological regions, medical image segmentation could assist clinicians in tracking the health of the patients by identifying abnormalities and planning treatments [16, 27]. This is performed by clinical experts who manually outline the borders for segmentation which can subsequently be used in deep learning algorithms. However, labeling medical images requires consensus of multiple clinical experts making it expensive and difficult, especially in resource-constrained settings. Few-shot learning and zero-shot learning prove to be very useful in such scenarios [15].

Over the past decade, a multitude of deep learning models, including U-Net [20], and transformer-based models such as TransUNet [7] and DAE-Former [3], have been developed for image segmentation tasks. The latest large-scale models (LM) such as GPT-4 [1], SAM [12], DALL-E [19] and SegGPT [23] provided a platform to solve different image segmentation tasks. These models are trained on huge datasets and the performance of these models is highly

*These authors contributed equally to this work

competitive even in zero-shot learning. However, resources such as memory and the compute required for training and fine-tuning these models for downstream tasks are significantly large making it difficult to deploy them in a resource-constrained setting. Although the SAM and SegGPT models show SOTA performances, these models are not trained on medical images and thus, cannot be utilized off-the-shelf for tasks like medical image segmentation. Hence, an efficient fine-tuning strategy is required to utilize the above-mentioned large-scale models for downstream tasks like medical image segmentation is required. There are several Parameter Efficient Fine-Tuning (PEFT) strategies which are categorized into additive, selective, reparameterized, and hybrid fine-tuning based on their operations [26]. In this work, we utilize SAM for the medical image segmentation task and adopt the Gradient Low-rank projection (**GaLore**) strategy to fine-tune it on medical image segmentation data [28]. We summarize our contributions in the following points:

1. We demonstrate **Medical Segment Anything Model with GaLore (MedSAGa)**, a framework integrating the Gradient Low-rank Projection (GaLore) optimization with SAM.
2. We perform rigorous experimentation on four diverse medical image segmentation datasets and compare the performance of MedSAGa with standard benchmarks in few-shot settings.
3. Our results showcase the significance of our framework by demonstrating notable reductions in memory over existing models while delivering comparable performance.

2. Related Works

A major milestone for medical image segmentation was achieved by developing U-Net, a model based on convolutional neural networks. Its novel architecture provides precise medical image segmentation even when trained on a limited number of images [20]. Further, several different variations of U-Net have been developed like DenseUNet [5] and ResUNet [18], which improved the segmentation performance by making significant changes in the structure of the U-Net architecture. The TransUNet model proposed in study [7] utilizes the transformer architecture for encoding in conjunction with the U-Net architecture [6]. It benefits from the global contextual information reception capabilities of transformers, that U-Net’s convolutional layers lack due to their local receptive fields. However, transformers require substantial computational resources, particularly in terms of GPU memory, because they process the entire image as a sequence of patches [8]. This sequential processing leads to high memory demands, especially when handling larger images typical in medical imaging applications. The hybrid nature of TransUNet, which combines convolutional operations with transformer mechanisms, in-

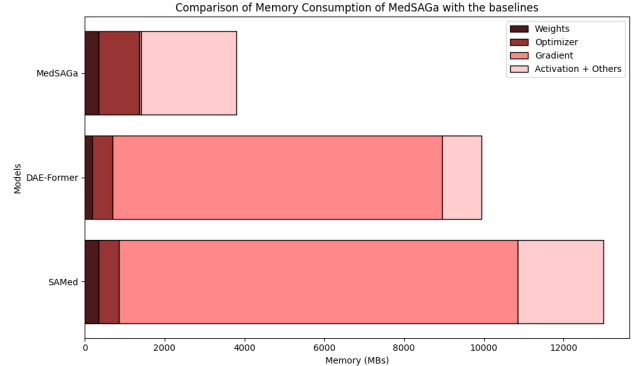


Figure 1. Memory consumption of MedSAGa and the other standard baselines while fine-tuning them for medical image segmentation task.

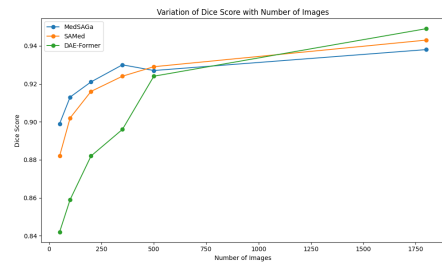


Figure 2. Dice Score vs Number of images while fine-tuning on ChestX-ray8 dataset. Here, for most models, the graph plateaus out at approximately 500 images.

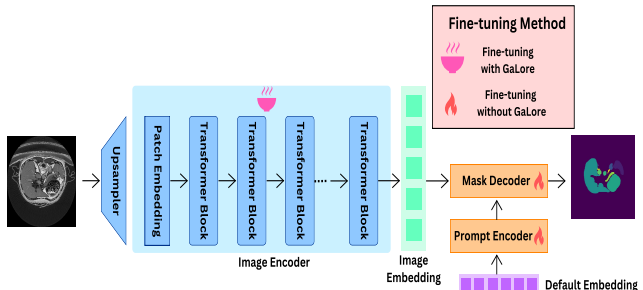


Figure 3. The architecture of MedSAGa. GaLore optimization is applied to fine-tune only the image encoder. Due to their lightweight characteristics, the Mask Decoder and the default embeddings of the Prompt Encoder are fine-tuned directly on the medical images without applying GaLore.

creases the complexity of the model. This complexity can make the training process more computationally intensive [7]. Further, the transformer layers in TransUNet require multiple self-attention calculations which are computationally expensive, especially for higher resolution inputs [7]. Due to the complexity and larger number of parameters, training TransUNet can be time and resource-consuming. This is exacerbated when fine-tuning on specific tasks as transformers generally take longer to train than their purely

convolutional counterparts. The use of advanced data augmentation and training strategies necessary to achieve optimal performance further extends the training duration and computational expense of TransUNet [7]. An architecture based on transformers, called DAE-Former [3], was further proposed, which utilizes an efficient dual attention mechanism and has been demonstrated to be better than TransUNet in terms of both computational efficiency and accuracy. However, the self-attention mechanism of DAE-Former, although redesigned for efficiency, still retains the intrinsic quadratic computational complexity with respect to the number of tokens. This complexity can lead to significant computational overhead when processing large datasets typical in medical imaging [3]. Thus, although these models prove to be quite efficient in image segmentation when trained for a particular task, for a diverse and resource-constrained domain such as healthcare, a generalized large-scale model capable of few-shot learning should be the most practical framework.

In the domain of large-scale free lunch models for image segmentation, SAM (Segment Anything Model) represents a significant milestone, trained on an extensive corpus of over 1B masks from 11M images [12]. It is noted for its superior performance, especially in zero-shot settings where it performs similarly to or even better than many supervised models. However, SAM doesn't perform well on medical image segmentation as it is trained on natural images and hence, cannot capture the semantics required in medical image segmentation [13]. After fine-tuning the SAM model for medical image segmentation task, SAM shows promising few shot learning results [17].

Parameter Efficient Fine-tuning (PEFT) techniques provide a solution for adapting such large-scale models for downstream tasks by reducing the number of trainable parameters while maintaining comparable performance [25]. One such approach, known as LoRA (Low-Rank Adaptation) does this by freezing the pre-trained model weights and integrating low-rank matrices into the transformer layers [10]. This significantly reduces the number of trainable parameters required for fine-tuning the large-scale models for various downstream tasks. A medical image segmentation model, SAMed (Customized Segment Anything Model for Medical Image Segmentation) utilizes these LoRA layers for fine-tuning the image encoder of SAM [26]. It further updates the prompt encoder and mask decoder parameters on medical image segmentation datasets which enhances the segmentation capability of SAM on medical images. This approach provides significant improvement in performance while utilizing less memory for fine-tuning on medical images [26].

A novel approach to reducing memory consumption was introduced in **GaLore** (Gradient Low-Rank Projection) [28] which presents a memory-efficient technique for fine-tuning

transformer-based models by projecting gradients into a low-rank space during training. This method effectively reduces the memory footprint of optimizer states while preserving the capability to learn full-rank weights. As a result, GaLore enables more efficient training on consumer-grade GPUs without the necessity for model parallelism or checkpointing. In our framework, MedSAGa, we leverage GaLore for fine-tuning the SAM architecture, showcasing its effectiveness in medical image segmentation, particularly in resource-constrained environments.

3. Methodology

3.1. Overview

Through MedSAGa, our primary aim is to harness the few-shot capabilities of a large-scale image segmentation model such as SAM and apply it to a resource-constrained setting like healthcare [4]. As seen in fig. 1, MedSAGa is more efficient than most SOTA models in both the training as well as inferencing stage (which uses *weights+activations+others* memory). By resource-constrained settings, we refer to the requirement of a substantially less number of annotated data to train or fine-tune the segmentation models and an inability to procure huge memory and computational resources required to train large-scale models. SAMed attempted to address this by integrating LoRA layers into its image encoder [26], however, it still requires huge memory and computational resources while facing the challenge of not utilizing the entire parameter matrix for training. Hence, in our work **MedSAGa**, we demonstrate a more refined approach to adapt SAM in resource-constrained settings by applying **GaLore** to all the parameters of the image encoder and then fine-tuning it, which significantly reduces the memory and computational cost while still maintaining full parameter structure. In addition to this, we fine-tune the prompt encoder and mask decoder without GaLore to perform improved semantic segmentation on medical images, as is demonstrated in SAMed [26]. We note here that since the prompt encoder and mask decoder in SAM are lightweight [26], applying GaLore for fine-tuning them would not lead to a substantial improvement in memory consumption. Fig. 1 shows the memory utilization by MedSAGa and the other SOTA models while fine-tuning on medical images. Furthermore, as seen in fig. 2, it can be observed that after a specific number of images, the performance graph plateaus out supporting the idea to use few-shot learning in resource constrained settings giving very close performance to using the entire dataset while using a smaller proportion of images.

SAM generates multiple segmentation masks to avoid ambiguity. However, we align MedSAGa with the working of SAMed and generate multiple segmentation masks, each representing a different tissue or segment of the anatomy in

addition to the background mask. These masks are then further post-processed to give the final segmentation result. For the training phase, we adopt warmup to stabilize the training process and use the AdamW optimizer for improved performance as was suggested in the SAMed architecture [26].

3.2. The Architecture

To reduce the resources required for utilizing SAM, we apply GaLore optimization to all the parameters of the image encoder. This approach harnesses the gradually changing low-rank structure of the gradient explained in the GaLore paper, which improves memory efficiency while still giving comparable results [28]. Instead of reducing the weight parameter size as is done in LoRA, GaLore projects the Gradient matrix at time t , $G_t \in \mathbb{R}^{m \times n}$, into a low-rank matrix \tilde{G}_t , which can be represented by eq. 1.

$$\tilde{G}_t = P_t \rho_t (P_t^\top G_t Q_t) Q_t^\top. \quad (1)$$

where P_t and Q_t are projection matrices with dimensions $\mathbb{R}^{m \times r}$ and $\mathbb{R}^{n \times r}$ respectively, and ρ_t is an element-wise stateful gradient regularizer. If W_0 is the initial weight matrix, W_T represents the weight matrix at time T , and η is the learning rate, then the gradient update rule in GaLore is as follows in eq. 2.

$$W_T = W_0 + \eta \sum_{t=0}^{T-1} \tilde{G}_t. \quad (2)$$

In our approach, we apply this Gradient low-rank projection to all the parameters of the image encoder which includes all the projection layers (q , k , v and o) as opposed to SAMed which applies LoRA only to the q and v projection layers in its best-performing model. We apply GaLore to all the parameters of the Image encoder as it adds only a negligible memory overhead. For the MedSAGa approach to function as an auto-segmentation model, we do not provide any prompts to the prompt encoder. Instead, we utilize the default embedding of the prompt encoder of SAM, which it uses when no prompt is given, and only fine-tune it during the training phase.

The mask decoder of SAM consists of a lightweight transformer layer and a segmentation head [26]. In our approach, we fine-tune the entire mask decoder directly without applying any optimization as it is already lightweight. Furthermore, as was developed in the SAMed architecture, we change the segmentation head of the mask decoder to adapt it to give precise semantic segmentation for each class of tissue or anatomy present in the image. Let us consider there are k classes in total including 1 background class in the medical image, the mask decoder of MedSAGa predicts k segmentation masks $M \in \mathbb{R}^{h \times w \times k}$, each corresponding to a single class in the image. We then further utilize a

combination of *argmax* and *softmax* functions to generate a segmentation map \hat{Y} as shown in eq. 3 where $d = -1$ represents the channel dimensions..

$$\hat{Y} = \operatorname{argmax}(\operatorname{Softmax}(M, d = -1), d = -1) \quad (3)$$

These adjustments make MedSAGa is an easy to implement solution in the SAM architecture with minimal engineering required, thereby making our solution very practical and adaptable for varied settings.

3.3. Training Strategies

For performing training, we utilize a combination of Cross Entropy loss and Dice loss, similar to that utilized in the SAMed approach as represented by the eq. 4.

$$\mathcal{L} = \lambda \mathcal{L}_{CE}(M, D(S)) + (1 - \lambda) \mathcal{L}_{Dice}(M, D(S)), \quad (4)$$

where \mathcal{L} represents the net loss value, \mathcal{L}_{CE} represents the Cross Entropy loss, \mathcal{L}_{Dice} represents the Dice loss and λ represents the loss weight. D represents downsampling to align the resolution of the ground truth mask (S) with the MedSAGa output, compensating for lower spatial resolution of MedSAGa.

Warmup is applied in MedSAGa to stabilize the training process. By allowing the learning rate to increase gradually, we enable the model to slowly adapt the weights to the specific characteristics of the medical data, thereby avoiding poor convergence and instability early in the training phase and reducing the chances of overfitting [24].

Instead of Adam optimizer, in MedSAGa we utilize the AdamW optimizer. AdamW decouples weight decay from the gradient updates and applies it directly to the weights. This method proves to be more effective in regularization, maintaining a better separation between the weight decay and the adaptive learning rate aspects of Adam [14]. In MedSAGa, the AdamW approach ensures that the regularization is not overly influenced by the learning rate adaptations specific to different weights.

4. Experiments and Results

We demonstrate the performance of MedSAGa through rigorous experimentation on 4 different medical datasets by comparing it to several baseline models.

4.1. Datasets and Evaluation Metrics

Datasets. We utilize four different datasets covering different parts of the human anatomy for our experimentation. All the baselines and results that we present in the further sections have been tested on each of these 4 datasets to evaluate the robustness of the MedSAGa architecture. For each dataset, the number of few-shot images used for experimentation are chosen depending upon the size of the dataset and the number of classes.

The *AMOS dataset* is a large-scale clinical dataset of 500 MRI and 100 CT scans which consists of annotations of 15 abdominal organs [11]. Each slice was padded to obtain final slices of dimension 512×512 . For the training set, we only considered the slices that had masks of at least 5 organs to overcome class imbalance. In total, 10,300 slices were satisfying the above criteria out of which we used 500, 1000, 2000, 5000, and 7000 slices for the few shot experimentation. The *ChestX-ray8 dataset* consists of 108,948 frontal-view X-ray images of 32,717 unique patients [22]. The images consist of 8 labels, mined from the text corpus of the corresponding radiological reports using NLP. We predict the segmentations for three classes whose masks were available: left lung, right lung and heart. Out of the 108,948 images in the dataset, we used only 50, 100, 200, 350, 500 and 1800 images as performance saturation was reached at quite an early stage (Refer Fig. 2). The *Ischemic Stroke Lesion Segmentation (ISLES) dataset* is a multi-center MRI dataset of acute to subacute stroke lesions [9]. It consists of 400 multi-vendor MRI images, each consisting of a number of slices having a dimension of 112×112 . The DWI modality was used for experimentation and as a pre-processing step, thresholding was applied to only use slices containing lesions while training. For performing few-shot experiments, 200, 500, 700, 1000, 2000 and 3,200 (maximum number of slices obtained after thresholding) slices were used in the ISLES dataset. The *Spleen dataset* was retrieved from the Medical Segmentation Decathlon challenge [2]. It consists of 61 3D volume portal-venous phase CT scans from patients undergoing treatment for liver metastases. Out of these, we utilize only those images for training that have a mask available. Data leakage between the train and test sets was avoided by splitting the data according to the patients instead of according to individual slices for all datasets.

Evaluation Metrics We use dice score and HD95 metrics to compare the model performances. Also, we show the memory utilized by the model for training and fine tuning.

4.2. Implementation details and evaluation metrics

All the experiments were run on a single NVIDIA RTX A6000 GPU with 48GB GPU RAM. A batch size of 12 was used for all the experiments. The warmup and loss weight strategies were the same as used in SAMed, i.e., the loss weights for cross entropy and dice loss were set to 0.2 and 0.8, respectively. For the warmup, the initial learning rate was set to 0.005, while the warmup period was set to 250. The β_1 , β_2 , and the weight decay of the AdamW optimizer were set to 0.9, 0.999, and 0.1, respectively. For the GaLore optimizer, AdamW was used as the base optimizer with a learning rate of 1×10^{-3} , and β_1 and β_2 were set to 0.9 and 0.999, respectively. The plane change rate (T) used was 200, as is recommended in the GaLore Paper. The

Table 1. Results of segmentation performances across datasets

No. of Images	MedSAGa		SAMed		DAE-Former	
	Dice	hd95	Dice	hd95	Dice	hd95
Chest-Xray Dataset						
50	0.899	44.704	0.882	48.772	0.842	183.220
100	0.913	39.430	0.902	39.361	0.859	130.535
200	0.921	33.745	0.916	34.372	0.882	98.342
350	0.930	29.235	0.924	30.421	0.896	72.783
500	0.934	30.502	0.929	27.764	0.924	43.698
1800	0.938	24.456	0.943	21.652	0.949	19.986
ISLES Dataset						
200	0.343	11.988	0.218	26.736	0.267	14.296
500	0.537	12.840	0.227	22.560	0.435	19.890
700	0.534	11.011	0.280	20.140	0.553	13.919
1000	0.574	8.900	0.368	20.690	0.546	12.774
2000	0.685	6.953	0.686	6.953	0.683	9.962
3200	0.783	3.748	0.742	14.977	0.733	11.019
Spleen Dataset						
100	0.842	14.645	0.807	15.836	0.793	20.029
200	0.838	13.598	0.869	10.861	0.877	39.166
500	0.882	12.006	0.877	10.473	0.905	26.740
700	0.876	12.176	0.878	4.643	0.901	12.290
800	0.882	15.851	0.907	49.979	0.916	26.016
AMOS Dataset						
500	0.199	66.697	0.166	71.604	0.268	101.784
1000	0.208	64.047	0.201	68.203	0.301	93.830
2000	0.222	68.311	0.201	67.397	0.299	92.947
5000	0.314	79.729	0.250	62.494	0.314	85.232
7000	0.389	52.768	0.377	56.124	0.349	79.323

base pre-trained model architecture for training our SAM-based model was the `vit_b` model, which occupies 5.25% (18.81M) of the original model size (358M).

Table 2. Comparison of segmentation performance of MedSAGa on the Spleen dataset, when fine-tuned with and without using warmup on Chest X-ray dataset.

Dataset	With Warmup		Without warmup	
	Mean Dice	Mean HD95	Mean Dice	Mean HD95
<i>Spleen(500img)</i>	0.882	12.006	0.858	18.731
<i>ISLES(200img)</i>	0.343	11.988	0.083	12.112
<i>CXR(100img)</i>	0.913	39.430	0.736	109.502
<i>AMOS(500img)</i>	0.199	66.697	0.196	68.014

4.3. Comparison with SOTA

The results of the memory utilization by MedSAGa and other baselines are depicted in Fig. 1. From this it is evident that the MedSAGa model utilizes the lowest memory as compared to the other SOTA image segmentation models, giving an average memory efficiency of 66% more as compared to current state-of-the-art (SOTA) models for medical image segmentation. Here, we would like to mention that

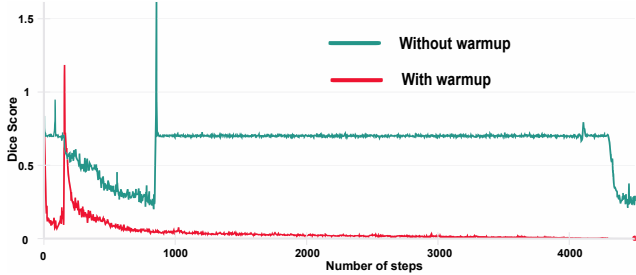


Figure 4. Comparison of loss curves between fine-tuning with and without applying warmup on ChestX-ray8 dataset.

Table 3. Ablation Studies of variations in fine-tuning SAM architecture with GaLore

Dataset	No. of Images	Medsaga		Medsaga_v1		Medsaga_v2	
		Dice	hd95	Dice	hd95	Dice	hd95
Chest-Xray	50	0.899	44.704	0.703	138.368	0.119	492.937
	1800	0.943	24.456	0.876	57.477	0.119	492.937
ISLES	200	0.343	11.988	0.415	16.011	0.007	59.111
	3200	0.783	3.748	0.783	3.748	0.007	59.111
Spleen	100	0.842	14.645	0.439	30.209	0.006	295.004
	800	0.882	15.851	0.471	29.551	0.006	295.004
AMOS	500	0.199	66.696	0.198	90.752	0.016	231.947
	7000	0.359	52.768	0.325	90.058	0.016	231.947

since the memory utilization reported in the Fig. 1 are the model memories, they are independent of the training data and depend only on the model parameters. Hence, MedSAGa is highly memory efficient as compared to the other standard baselines in both training and inferencing phases.

The results of the segmentation performance are compiled in the Table 1. The table shows the performance metrics, the mean Dice Scores and the mean HD95 scores, for various few-shot settings across the four medical image datasets. These results depict the ability of **MedSAGa** as the best approach in terms of memory efficiency while still giving comparable segmentation performances in most of the settings. In the domain of SAM-based models for medical image segmentation, we beat the state-of-the-art model, SAMed not only in terms of memory efficiency but also in segmentation performance in almost every few shot settings across all datasets.

Comparing with DAE-Former, MedSAGa performs better segmentation in very low resource settings for most datasets like Chest X-ray, ISLES and Spleen datasets with a slight drop in the dice score when higher number of training images are used. Furthermore, MedSAGa utilizes 61% less memory compared to DAE-Former.

5. Ablation Studies

We present our ablation studies in two categories. In the first part, we demonstrate two variations of integrating Gradient

low-rank projection optimization in the MedSAGa architecture. In the first variation (referred to as *MedSAGa_v1*), we apply the GaLore optimization only to the attention parameters of the image encoder for fine-tuning and the prompt encoder and mask decoder are fine-tuned without using GaLore. Even though GaLore is only applicable to the immediate attention layer succeeding MLP layer of the transformer neural network, we apply it on all the attention parameters in ViT of SAM to justify the same. In the second variation (referred to as *MedSAGa_v2*), we apply GaLore to all the parameters of the image encoder and fine-tune it and do not perform any fine-tuning on the prompt encoder and mask decoder. Both these variations were tested on the Chest X-ray dataset and the results of MedSAGa_v1, MedSAGa_v2 along with the best-performing model, MedSAGa are presented in Table ???. Our second category of ablation studies is based on experimenting with the effects of applying warmup while fine-tuning MedSAGa. Fig. 4 shows the results of segmentation performance on all the datasets when fine-tuned with and without warmup. The results of the same study on other datasets is mentioned in the supplementary material.

6. Limitations and Future Scope

The MedSAGa methodology leverages a large-scale model akin to SAM for few-shot image segmentation within resource-constrained environments, exhibiting a marked reduction in memory utilization compared to other SOTA models, while still yielding comparable segmentation performance. However, attaining optimal segmentation performance with MedSAGa may not always be feasible, as varying architectural designs may excel in capturing the distinctive features of diverse datasets. Additionally, as highlighted in the GaLore literature, further improvements in memory overhead can be achieved by reducing the projection layer dimensions via techniques such as quantization and streamlined parameterization, which can be done as part of the future work. Since this work presents SAM in culmination with GaLore (a gradient low-rank optimization technique) it can be applied to various end-to-end training techniques of models involving ViTs. Not just image segmentation, the use of GaLore alongside ViT can be interestingly used for a wide-variety of downstream tasks in a resource-constraint environments.

7. Conclusion

In our work, we demonstrate the use of large-scale models like SAM for few-shot medical image segmentation in resource-constrained settings like healthcare by using Gradient low-rank projection (GaLore) for fine-tuning the image encoder. This allows us to achieve significant memory efficiency while still utilizing full parameter training. Our rigorous experiments on diverse medical image seg-

mentation datasets showcase our approach’s effectiveness in resource-constrained environments. Easy integration with SAM architecture proves the practicality and efficiency of MedSAGa for healthcare implementation.

References

- [1] Josh Achiam, Steven Adler, Sandhini Agarwal, Lama Ahmad, Ilge Akkaya, Florencia Leoni Aleman, Diogo Almeida, Janko Altmenschmidt, Sam Altman, Shyamal Anadkat, et al. Gpt-4 technical report. *arXiv preprint arXiv:2303.08774*, 2023.
- [2] Michela Antonelli, Annika Reinke, Spyridon Bakas, Keyvan Farahani, Annette Kopp-Schneider, Bennett A Landman, Geert Litjens, Bjoern Menze, Olaf Ronneberger, Ronald M Summers, et al. The medical segmentation decathlon. *Nature communications*, 13(1):4128, 2022.
- [3] Reza Azad, René Arimond, Ehsan Khodapanah Aghdam, Amirhossein Kazerouni, and Dorit Merhof. Dae-former: Dual attention-guided efficient transformer for medical image segmentation. In *International Workshop on PRedictive Intelligence In MEdicine*, pages 83–95. Springer, 2023.
- [4] Mélanie Bernhardt, Daniel C Castro, Ryutaro Tanno, Anton Schwaighofer, Kerem C Tezcan, Miguel Monteiro, Shruthi Bannur, Matthew P Lungren, Aditya Nori, Ben Glocker, et al. Active label cleaning for improved dataset quality under resource constraints. *Nature communications*, 13(1):1161, 2022.
- [5] Yue Cao, Shigang Liu, Yali Peng, and Jun Li. Denseunet: densely connected unet for electron microscopy image segmentation. *IET Image Processing*, 14(12):2682–2689, 2020.
- [6] Roberto Castro, Leo Ramos, Stady Román, Mike Bermeo, Anthony Crespo, and Erick Cuenca. U-net vs. transunet: Performance comparison in medical image segmentation. In *International Conference on Applied Technologies*, pages 212–226. Springer, 2022.
- [7] Jieneng Chen, Yongyi Lu, Qihang Yu, Xiangde Luo, Ehsan Adeli, Yan Wang, Le Lu, Alan L Yuille, and Yuyin Zhou. Transunet: Transformers make strong encoders for medical image segmentation. *arXiv preprint arXiv:2102.04306*, 2021.
- [8] Alexey Dosovitskiy, Lucas Beyer, Alexander Kolesnikov, Dirk Weissenborn, Xiaohua Zhai, Thomas Unterthiner, Mostafa Dehghani, Matthias Minderer, Georg Heigold, Sylvain Gelly, Jakob Uszkoreit, and Neil Houlsby. An image is worth 16x16 words: Transformers for image recognition at scale. In *International Conference on Learning Representations*, 2021.
- [9] Moritz R Hernandez Petzsche, Ezequiel de la Rosa, Uta Hanning, Roland Wiest, Waldo Valenzuela, Mauricio Reyes, Maria Meyer, Sook-Lei Liew, Florian Kofler, Ivan Ezhov, et al. Isles 2022: A multi-center magnetic resonance imaging stroke lesion segmentation dataset. *Scientific data*, 9(1):762, 2022.
- [10] Edward J Hu, Yelong Shen, Phillip Wallis, Zeyuan Allen-Zhu, Yuanzhi Li, Shean Wang, Lu Wang, and Weizhu Chen. Lora: Low-rank adaptation of large language models. *arXiv preprint arXiv:2106.09685*, 2021.
- [11] Yuanfeng Ji, Haotian Bai, Chongjian Ge, Jie Yang, Ye Zhu, Ruimao Zhang, Zhen Li, Lingyan Zhanng, Wanling Ma, Xiang Wan, et al. Amos: A large-scale abdominal multi-organ benchmark for versatile medical image segmentation. *Advances in Neural Information Processing Systems*, 35:36722–36732, 2022.
- [12] Alexander Kirillov, Eric Mintun, Nikhila Ravi, Hanzi Mao, Chloe Rolland, Laura Gustafson, Tete Xiao, Spencer Whitehead, Alexander C. Berg, Wan-Yen Lo, Piotr Dollar, and Ross Girshick. Segment anything. In *Proceedings of the IEEE/CVF International Conference on Computer Vision (ICCV)*, pages 4015–4026, 2023.
- [13] Tianang Leng, Yiming Zhang, Kun Han, and Xiaohui Xie. Self-sampling meta sam: Enhancing few-shot medical image segmentation with meta-learning. In *Proceedings of the IEEE/CVF Winter Conference on Applications of Computer Vision*, pages 7925–7935, 2024.
- [14] Ilya Loshchilov and Frank Hutter. Decoupled weight decay regularization. In *International Conference on Learning Representations*, 2019.
- [15] Ziqian Lu, Zheming Lu, Yunlong Yu, and Zonghui Wang. Learn more from less: Generalized zero-shot learning with severely limited labeled data. *Neurocomputing*, 477:25–35, 2022.
- [16] Jun Ma, Yuting He, Feifei Li, Lin Han, Chenyu You, and Bo Wang. Segment anything in medical images. *Nature Communications*, 15(1):654, 2024.
- [17] Maciej A Mazurowski, Haoyu Dong, Hanxue Gu, Jichen Yang, Nicholas Konz, and Yixin Zhang. Segment anything model for medical image analysis: an experimental study. *Medical Image Analysis*, 89:102918, 2023.
- [18] Hameedur Rahman, Tanvir Fatima Naik Bukht, Azhar Imran, Junaid Tariq, Shanshan Tu, and Abdulkareem Alzahrani. A deep learning approach for liver and tumor segmentation in ct images using resunet. *Bioengineering*, 9(8):368, 2022.
- [19] Aditya Ramesh, Mikhail Pavlov, Gabriel Goh, Scott Gray, Chelsea Voss, Alec Radford, Mark Chen, and Ilya Sutskever. Zero-shot text-to-image generation. In *International conference on machine learning*, pages 8821–8831. Pmlr, 2021.
- [20] Olaf Ronneberger, Philipp Fischer, and Thomas Brox. U-net: Convolutional networks for biomedical image segmentation. In *Medical Image Computing and Computer-Assisted Intervention – MICCAI 2015*, pages 234–241, Cham, 2015. Springer International Publishing.
- [21] Risheng Wang, Tao Lei, Ruixia Cui, Bingtao Zhang, Hongying Meng, and Asoke K Nandi. Medical image segmentation using deep learning: A survey. *IET Image Processing*, 16(5):1243–1267, 2022.
- [22] Xiaosong Wang, Yifan Peng, Le Lu, Zhiyong Lu, Mohammadhadi Bagheri, and Ronald M Summers. Chestx-ray8: Hospital-scale chest x-ray database and benchmarks on weakly-supervised classification and localization of common thorax diseases. In *Proceedings of the IEEE conference on computer vision and pattern recognition*, pages 2097–2106, 2017.
- [23] Xinlong Wang, Xiaosong Zhang, Yue Cao, Wen Wang, Chunhua Shen, and Tiejun Huang. Seggpt: Towards seg-

- menting everything in context. In *Proceedings of the IEEE/CVF International Conference on Computer Vision (ICCV)*, pages 1130–1140, 2023.
- [24] Ruibin Xiong, Yunchang Yang, Di He, Kai Zheng, Shuxin Zheng, Chen Xing, Huishuai Zhang, Yanyan Lan, Liwei Wang, and Tieyan Liu. On layer normalization in the transformer architecture. In *International Conference on Machine Learning*, pages 10524–10533. PMLR, 2020.
- [25] Lingling Xu, Haoran Xie, Si-Zhao Joe Qin, Xiaohui Tao, and Fu Lee Wang. Parameter-efficient fine-tuning methods for pretrained language models: A critical review and assessment. *arXiv preprint arXiv:2312.12148*, 2023.
- [26] Kaidong Zhang and Dong Liu. Customized segment anything model for medical image segmentation. *arXiv preprint arXiv:2304.13785*, 2023.
- [27] Yichi Zhang, Zhenrong Shen, and Rushi Jiao. Segment anything model for medical image segmentation: Current applications and future directions. *Computers in Biology and Medicine*, page 108238, 2024.
- [28] Jiawei Zhao, Zhenyu Zhang, Beidi Chen, Zhangyang Wang, Anima Anandkumar, and Yuandong Tian. Galore: Memory-efficient llm training by gradient low-rank projection. *arXiv preprint arXiv:2403.03507*, 2024.